INTERACTION OF EMODIN AND ITS DERIVATIVE FRANGULIN-A WITH BOVINE SERUM ALBUMIN AND CALF THYMUS DNA

X.-X. Hu [1], Zh.-F. Huang [1], G.-Sh. Lu [1,2*], J.-Y. Huang [1], X. Tan [1], G.-T. Huang [3]

[1] Guangxi Institute of Traditional Medical and Pharmaceutical Sciences, Nanning, 530022, China; e-mail: huxiaoxi0124@126.com
[2] Guangxi Key Laboratory of Traditional Chinese Medicine Quality Stardands, Nanning, 530022, China
[3] Reproductive Medicine Center, Maternal and Child Health Hospital of Guangxi Zhuang Autonomous Region, 530004, Nanning, China

The interaction between emodin, frangulin-A (obtained from Ventilago leiocarpa Benth) with bovine serum albumin (BSA) and calf thymus DNA (ct-DNA) has been investigated. The fluorescence spectrum and molecular docking methods are used to investigate the interaction between emodin, frangulin-A, and BSA. The UV spectrum revealed interaction between emodin, frangulin-A, and ct-DNA. The fluorescence spectrum confirmed that the compounds of emodin–BSA and frangulin-A–BSA were formed showing fluorescence quenching and a decrease of the maximum emission wavelength. The simulated molecular docking showed stable combinations of emodin–BSA and frangulin-A–BSA. Thus, molecular interactions mainly occur due to hydrophobic forces and hydrogen bonds. According to the UV spectrum, emodin and frangulin-A interacted with ct-DNA via electrostatic interaction.

Keywords: *emodin, frangulin-A, Ventilago leiocarpa Benth, bovine serum albumin, calf thymus DNA.*

ВЗАИМОДЕЙСТВИЕ ЭМОДИНА И ЕГО ПРОИЗВОДНОГО ФРАНГУЛИНА-А С БЫЧЬИМ СЫВОРОТОЧНЫМ АЛЬБУМИНОМ И ДНК ТИМУСА ТЕЛЕНКА

X.-X. Hu [1], Zh.-F. Huang [1], G.-Sh. Lu [1,2*], J.-Y. Huang [1], X. Tan [1], G.-T. Huang [3]

УДК 535.372

[1] Институт традиционной медицины и фармацевтики Гуанси, Наньнин, 530022, Китай; e-mail: huxiaoxi0124@126.com
[2] Лаборатория стандартов качества традиционной китайской медицины Гуанси, Наньнин, 530022, Китай
[3] Центр репродуктивной медицины, Наньнин, 530004, Китай

(Поступила 22 октября 2018)

Исследовано взаимодействие эмодина, франгулина-А (полученного из Ventilago leiocarpa Benth) с бычьим сывороточным альбумином (БСА) и ДНК тимуса теленка (ct-ДНК). По спектрам УФ-поглощения выявлено взаимодействие между эмодином, франгулином-А и ct-ДНК. Спектры флуоресценции подтверждают, что соединения эмодин–БСА и франгулин-А–БСА демонстрируют тушение флуоресценции и уменьшение максимальной длины волны излучения. Молекулярный докинг показывает стабильные комбинации эмодин–БСА и франгулин-А–БСА. Молекулярные взаимодействия происходят в основном с участием гидрофобных сил и водородных связей. Эмодин и франгулин-А связываются с ct-ДНК посредством электростатического взаимодействия.

Ключевые слова: *эмодин, франгулин-А, Ventilago leiocarpa Benth, бычий сывороточный альбумин, ДНК тимуса теленка.*

Introduction. *Ventilago leiocarpa* Benth is rich in quinine compounds, such as emodin, physcion, ventilagolin, and ventiloquinone-I [1]. Modern pharmacology confirms that emodin shows better antineoplastic, hypotensive, and anti-inflammatory activities [2–4]. Frangulin-A is the 6-rhamnosyl glycoside of aglycone that uses emodin as the parent nucleus [5] (Fig. 1), mostly obtained from the roots or branches of the genus

rhamnolidae [6, 7]. Kurkin reported that frangulin-A and frangulin-B are the active compounds and elaborated methodical approaches to the standardization of frangula bark and anthracene derivatives [8]. Wei reported that frangulin-B exhibited potent inhibitory effects on the TNF-α formation of LPS/IFN-γ (interferon-γ)-stimulated murine microglial cell lines N9 [9].

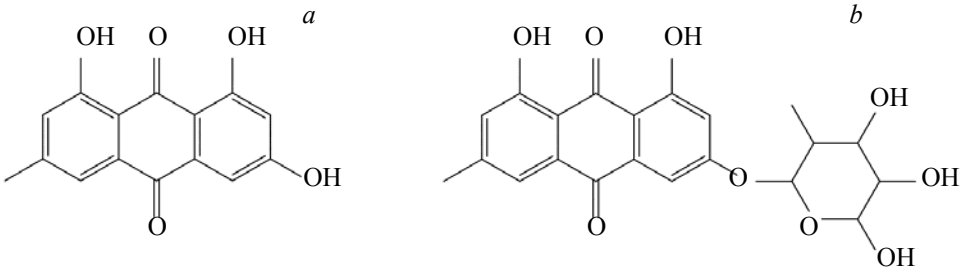

Fig. 1. Chemical structure of emodin (a) and frangulin-A (b).

Bovine serum albumin (BSA) is the main carrier protein in mammalian plasma, having the important function of storing and transporting exogenous small molecules [10]. When bioactive substances are absorbed into the body, serum albumin transports them through various physiological membranes to various tissues and organs [11], and the combination rate and ability of the two compounds are different [12]. Fluorescence quenching is an important method to study the effect of drugs on proteins [13]. Recently, the interaction between drugs and protein molecules has been studied by enhancing or decreasing fluorescence after adding drugs [14]. Meanwhile, calculation of the quenching constant permitted an understanding of the mechanism of interaction between drugs and proteins [15].

DNA is not just the carrier of genetic information but also the main receptor for most drug molecules [16]. DNA is the target molecule determining the drug effect [17, 18]. This study investigates the interaction of emodin and frangulin-A with BSA and ct-DNA to understand the binding mechanism of the compound with protein and DNA and provide clues to the nature of the binding phenomenon.

Experimental. *Ventilago leiocarpa* Benth was collected in Yulin, Guangxi, China, in August 2015 and identified by Professor of Pharmacy Wen-Jie Lu from the Guangxi Institute of Traditional Medical and Pharmaceutical Sciences. BSA was purchased from Shanghai Yuanye Bio-Technology, Tris(hydroxymethy) aminomethane (TRIS) is used as the buffer ct-DNA was from Biotope. The solutions of ct-DNA gave a UV absorbance ratio (260 over 280 nm) of more than 1.8, which indicated its purity. Petroleum ether and ethyl acetate were from Guanghua Sci-Tech, Guangdong, China. Deionized water was purified by Milli-Q Water.

Fluorescence spectroscopy was recorded on a RF-6000 fluorescence spectrophotometer (Shimadzu, Japan). The UV absorption spectrum was recorded on a UV2500PC UV spectrophotometer (Shimadzu, Japan).

Extraction and isolation. The dried medical material (10 kg) of *Ventilago leiocarpa* Benth was powdered and extracted three times with 95% EtOH. The extract was concentrated under reduced pressure to give a crude residue (3.56 kg), which was suspended in distilled water and extracted with ethyl acetate. Then, the ethyl acetate extract (112 g) was separated by the silica gel chromatography column with petroleum ether-ethyl acetate (9:1, v/v) as a mobile phase. Compounds **1** (4.6 g) and **2** (1.2 g) were obtained after repeating the reverse silica gel column chromatography and preparative high-performance liquid chromatography.

Protein binding studies. The BSA stock solution (1.0×10^{-4} M) was prepared in water. Experiments on the interaction of frangulin-A (5×10^{-4} M) complexes with BSA were carried out in 10 mM Tris-HCl (pH 7.4) buffer and stored at 4°C. All spectra were recorded after each successive addition of the compounds and incubation at room temperature for 15 min to complete the interaction.

Fluorescence quenching measurements. The BSA solution was fixed at 1.0×10^{-5} M and served as a blank control, and the concentration of the frangulin-A–BSA complex was 5–25 μM. The excitation and emission slit width was 3 nm and the wavelength resolution were at the nanometer level. The fluorescence spectrum was scanned in the range from 300 to 450 nm with a fixed excitation wavelength of 295 nm.

Synchronous fluorescence spectra. Synchronous fluorescence spectra were also recorded using the same concentration of BSA and complexes as mentioned above with two $\Delta\lambda$ (difference between the excitation and emission wavelengths of BSA) values of 15 and 60 nm.

Molecular simulation. The molecular docking calculations were performed by Discovery Studio 2.5 (DS). The structures of BSA (PDB ID: 3V03) were taken from the protein data bank (PDB). Before starting the

docking calculations, the water molecules from structures of frangulin-A and emodin were removed and polar hydrogen to protein was added. Protein molecules were defined as receptor molecules. The possible binding sites were discovered in the receptor using find sites from receptor cavities, the sphere was defined from the binding site, and the active radius was modified with ligand molecule minimization. After running molecular docking calculations, the diagram of ligand-protein interactions was built.

DNA binding studies. UV-Vis absorption titration can be used to investigate the interaction of frangulin-A with ct-DNA. ct-DNA with a constant concentration (1.0×10^{-4} M) and frangulin-A (1–6 μL, 1.0×10^{-5}M) were added to the quartz cell sequentially. The interval between each dosing was the same. At room temperature, the UV-Vis spectra of ct-DNA in the absence and presence of complexes were recorded in the range from 200 to 480 nm with a bandwidth of 1.5 nm. Tris-HCl (pH 7.4) buffer was used as a reference solution.

Results and discussion. Compound **1** was yellow fine needle-like crystals. It can be dissolved in sodium hydroxide solution with a red or purplish red color, but regaining the yellow color when the hydrochloric acid solution was added. Compared with the standard substance of emodin in thin-layer chromatography, the R_f values were consistent. Compound **1** was identified as emodin.

Compound **2** was orange fine needle-like crystals. EI-MS *m*/*z*: 416 $[M]^+$,^{1}H NMR (500 MHz, pyridine-d5) δ 7.74 (1H, s, H-7), 7.66 (1H, s, H-2), 7.30 (1H, s, H-5), 7.10 (1H, s, H-4), 6.30 (1H, s, H-1'), 4.75 (1H, s, H-5'), 4.66 (1H, d, J = 7.4 Hz, H-2'), 4.40 (1H, t, J = 9.1 Hz, H-4'), 4.28 – 4.19 (1H, m, H-3'), 2.24 (3H, s, H-15), 1.62 (3H, d, J = 5.8 Hz, H-6'). ^{13}C NMR (125 MHz, pyridine-d5) δ 191.33(C-9), 181.86 (C-10), 165.58 (C-1),164.30 (C-8), 163.03 (C-6), 149.19 (C-3), 136.00 (C-11), 133.88 (C-14), 124.95 (C-4), 121.65 (C-2), 114.35 (C-13), 111.57 (C-12), 110.35 (C-7), 109.90 (C-5), 100.41 (C-1'), 73.80 (C-4'), 72.65 (C-2'), 71.97 (C-3'), 71.83 (C-5'), 22.13 (C-15), and 18.92 (C-6'). The above data were consistent with those reported in the literature [19]. Compound **2** was identified as frangulin-A.

Fluorescence quenching refers to the decrease in the fluorescence intensity of a fluorophore due to the environmental alteration around the fluorophore, which can reveal the nature of the binding reaction [20, 21]. The fluorescence spectrogram of emodin–BSA and frangulin-A–BSA is presented in Fig. 2. BSA was excited at 295 nm in the fluorescence quenching measurements. When samples of different concentrations (5–25 μM) were added, the fluorescence intensity of BSA gradually decreased at 340 nm.

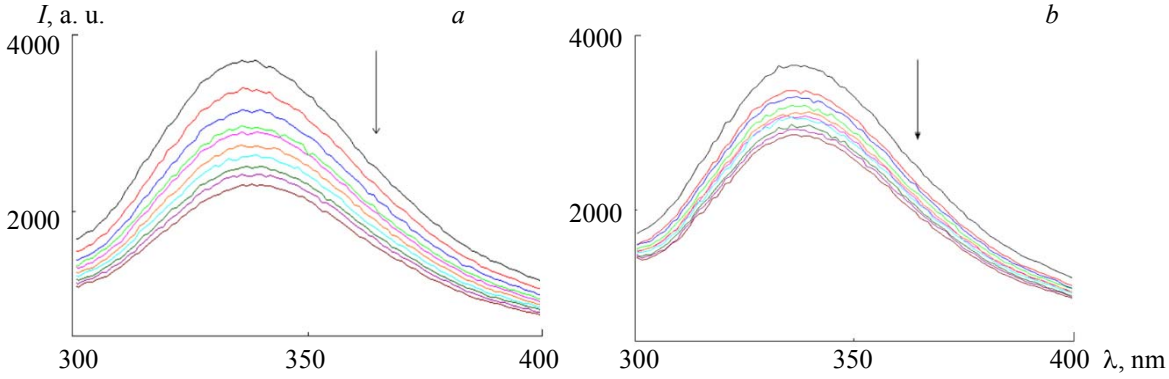

Fig. 2. Fluorescence spectra of emodin–BSA (a) and frangulin-A–BSA (b) complex.

The Stern–Volmer equation was used to quantitatively describe the magnitude of frangulin-A to quench the emission intensity of BSA:

$$F_0/F = 1 + K_q\tau_0\,[Q] = 1 + K_{SV}[Q], \quad (1)$$

where F_0 and F are the fluorescence intensities in the absence and presence of the quencher, respectively, Q is the quencher concentration. K_{SV} is the Stern–Volmer quenching constant, K_q is the biomolecular quenching rate constant, and τ_0 is the average lifetime of the fluorophore in the absence of the quencher (taken as 10^{-8} s [22]). As shown in Fig. 3 and Table 1, the plot exhibited a good linear relationship for three temperatures. The maximum scatter of the collision-quenching constant K_q of various quenchers for the biomacromolecule was about 2.0×10^{10} L · mol^{-1} · s^{-1} [23]. The above K_q values were all greater than the maximum scatter of the collision-quenching constant. The high temperature caused the dispersion coefficient to increase, so the quenching constant increased with increase in temperature. Dynamic quenching was caused

TABLE 1. Dynamic Fluorescence Quenching Parameters of Emodin and Frangulin-A with BSA

Compound	T, K	$K_{SV}/10^4$, L/mol	$K_q/10^{12}$, L·mol^{-1}·s^{-1}	R^2
Emodin	298	14.389	14.389	0.9260
	303	11.649	11.649	0.9954
	310	11.374	11.374	0.9942
Frangulin-A	298	1.552	1.552	0.9945
	303	1.298	1.298	0.9605
	310	1.259	1.259	0.9760

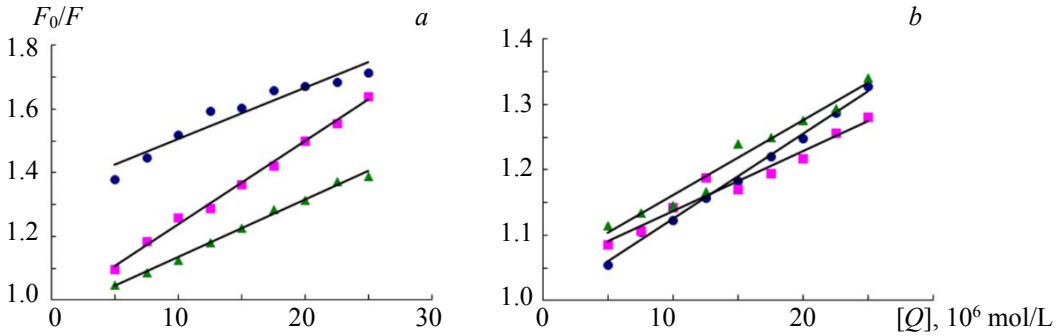

Fig. 3. Plot of F_0/F against [Q] of emodin (a) and frangulin-A (b), T = 298 (●), 303 (■), and 310 K (▲).

by molecular diffusion. As the temperature rose, the molecules collided faster. The constant of fluorescence quenching increased with increasing temperature. In static quenching, a complex between the quenching agent and the ground state of fluorescence formed. When the temperature rose, the compound became unstable, and the quenching constant decreased [24]. This indicated that the dominating quenching mechanism of emodin and frangulin-A was initiated by a static process, not by dynamic collision. The K_q value of emodin was significantly greater than that of frangulin-A, and the binding constant was much greater than that of the corresponding glycosides. The K_q value of 1,8-dihydroxyanthraquinone was greater than 1,8-dihydroxyanthraquinone glycoside [25].

The thermodynamic parameters for the binding of the drug molecule with biological macromolecules include hydrophobic interaction, Van der Waals force, electrostatic force, and the hydrogen bond. The values of the binding constant were determined at three different temperatures and shown in Table 1. When the temperature changed little, the reaction enthalpy was constant. The standard enthalpy change (ΔH) and standard entropy change (ΔS) have been estimated using the Van't Hoff equation:

$$\ln K = -\Delta H/RT + \Delta S/R, \quad (2)$$

where K is the binding constant at the corresponding temperature and R is the gaseous constant. The dependence $1/T = f(\ln K)$, ΔH, and ΔS are calculated from Eq. (2). The Gibbs free energy (ΔG) can be estimated from the following formula:

$$\Delta G = -RT\ln K_A = \Delta H - T\Delta S. \quad (3)$$

The negative value of ΔG at different temperatures (298, 303, and 310 K) reveals the spontaneity of the reaction, as shown in Table 2.

A spectrogram consisting of the fluorescence intensity and the corresponding excitation wavelength (or emission wavelength) is called a synchronous fluorescence spectrum (SFS). SFS shows the changes in the microenvironment around the fluorescent functional groups. As a rule, interactions between molecular probes and proteins are characterized by the difference between the excitation and emission wavelength. The different wavelengths of the synchro-fluorescence spectra showed the difference in the spectral characteristics of different amino acid residues. The maximum absorption wavelength of the amino acid residue depends on the polarity of the environment. While the ligand concentration increases, the redshift in the spectra indicates the increase in polarity of the environment in which the amino acid residues are located, and the blueshift indicates an increase in hydrophobicity.

TABLE 2. Thermodynamic Parameters of the Emodin–BSA and Frangulin-A–BSA System

Compound	T, K	ΔG, kJ/mol	ΔH, kJ/mol	ΔS, J·K^{-1}·mol^{-1}
Emodin	298	–46.261	15.526	158.646
	303	–48.054		
	310	–49.164		
Frangulin-A	298	–37.045	13.718	124.360
	303	–37.667		
	310	–38.538		

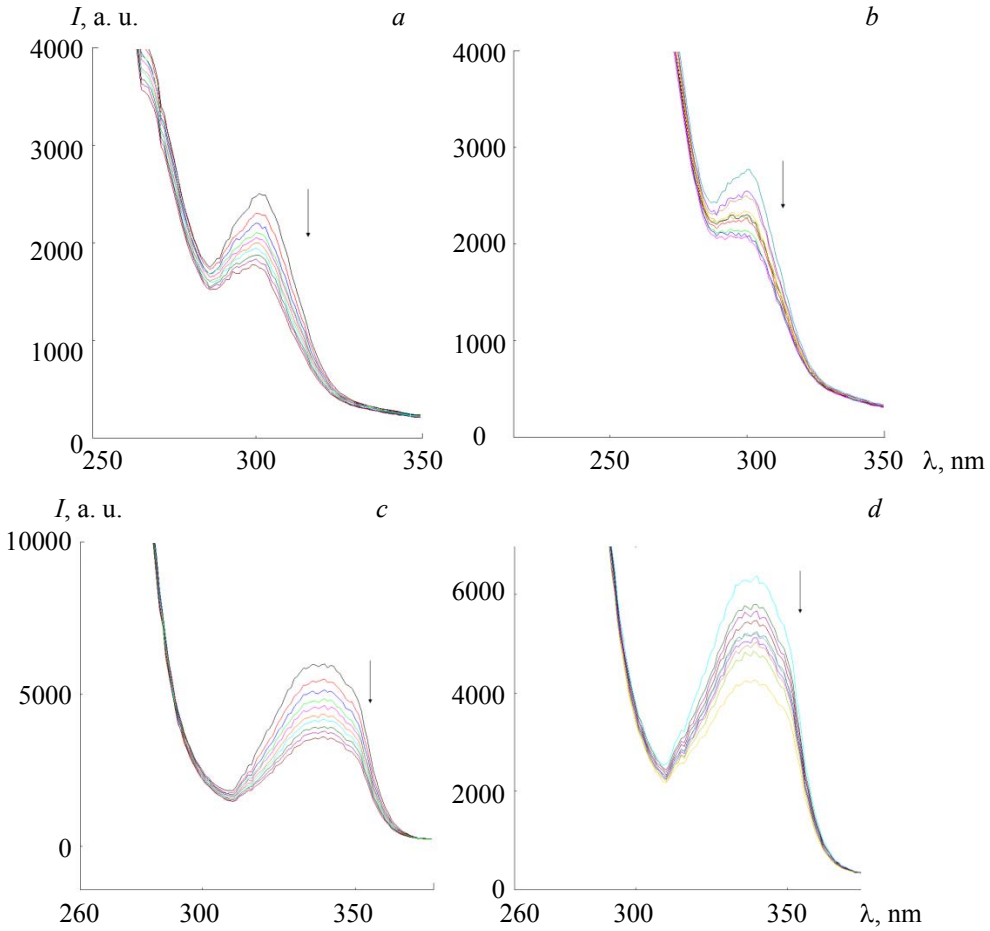

Fig. 4. Synchronous fluorescence spectra of interaction between BSA and emodin (a, c) and frangulin-A (b, d) for $\Delta\lambda$ = 15 (a, b) and 60 nm (c, d).

For $\Delta\lambda$ = 15 and 60 nm, the maximum emission wavelength for tryptophan was slightly blue-shifted in emodin–BSA and frangulin-A–BSA (Fig. 4). Owing to this, one can conclude that the hydrophobic amino acids were inserted into the cylinder to form hydrophobic cavities.

On the DS workstation the Libdock module is used. The 3D conformations of emodin and frangulin-A were minimized in energy. The comprehensive scoring was made by the docking mode affinity and the relative energy value of the ligand and the receptor. The 3D diagrams of molecular docking were drawn by selecting the highest conformation score of LibDockscore (Fig. 5). Linear analog molecules in BSA were the best docking conformations of emodin and frangulin-A, and the green dashed lines were hydrogen bonds.

In the Libdock, 2D planar diagrams of the interaction between emodin and frangulin-A and BSA were obtained by the draw-ligand-interaction-diagram (Fig. 6, Table 3). It was shown that for emodin, tryptophan (TRP213), arginine (ARG217), and valine (VAL342), three hydrogen bonds were formed. The spacing between emodin and tryptophan in BSA was longer but the binding ability was stronger [26]. Two glutamic

acids (GLU519), aspartic acid (ASP118) and proline (PRO117), formed four hydrogen bonds in frangulin-A. There were six amino acids (ARG198, ALA341, PRO446, TYR340, GLN220, and PRO338) participating in the hydrophobic interaction with emodin and five amino acids (PRO119, ASP178, THR514, LEU515, and PRO516) participating in the hydrophobic interaction with frangulin-A.

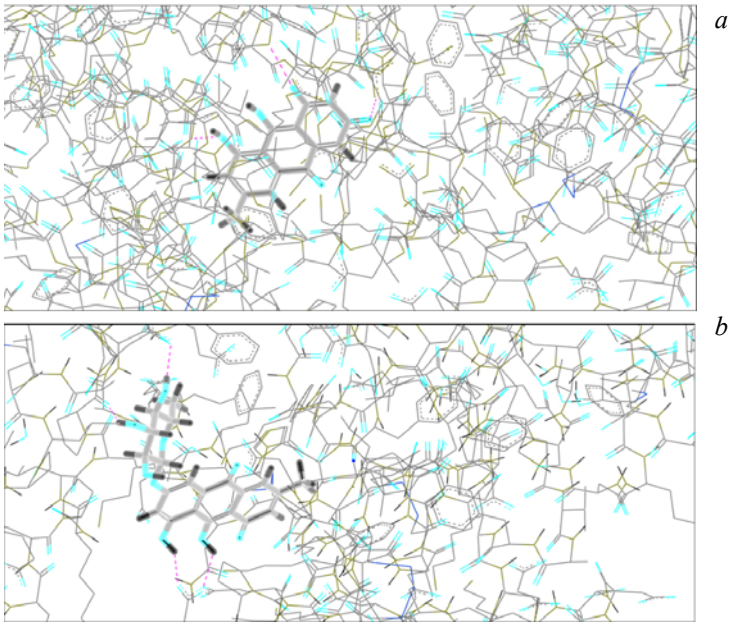

Fig. 5. Molecular docking 3D-disgram of BSA and emodin (a) or frangulin-A (b).

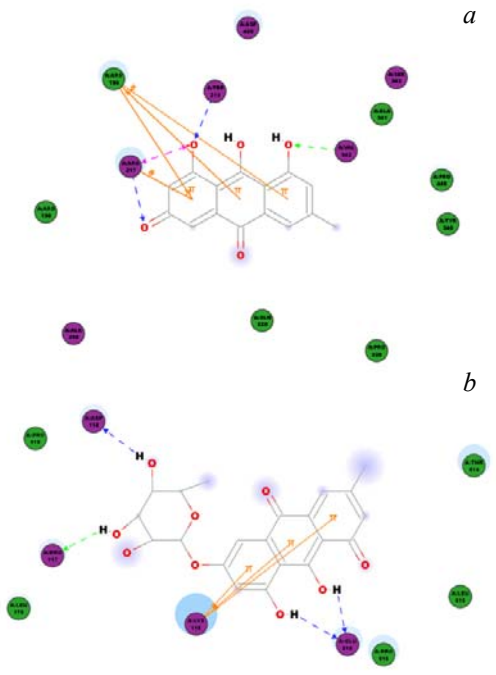

Fig. 6. 2D diagram of the molecular interaction between BSA and emodin (a) or frangulin-A (b).

The absorption spectra of emodin and frangulin-A in the absence and presence of ct-DNA (at constant concentrations of emodin and frangulin-A) are shown in Fig. 7. The absorption spectrum of the pure complex displays an intensive intraligand π-π^* transition at λ = 203 nm. When the molecules were inserted into

ct-DNA, the orbitals were didymous. The maximum absorption wavelength was redshifted as the concentration increased. The molecules interacted with ct-DNA in an electrostatic interaction. The peak of the spectrum did not change in location but changed in intensity.

TABLE 3. Hydrogen Bond Interaction between Emodin and Frangulin-A with BSA

Compound	No.	Ligand atom	Acceptor atom	Bond length×10^{-8} cm
Emodin	1	O19	TRP213:NE1	3.1377
	2	O20	ARG217:NH1	2.97101
	3	O15	VAL342:N	2.97448
Frangulin-A	1	H38	GLU519-OE1	2.4938
	2	H39	GLU519-OE2	2.07088
	3	H48	ASP118-OD1	2.343
	4	H49	PRO117-O	2.16344

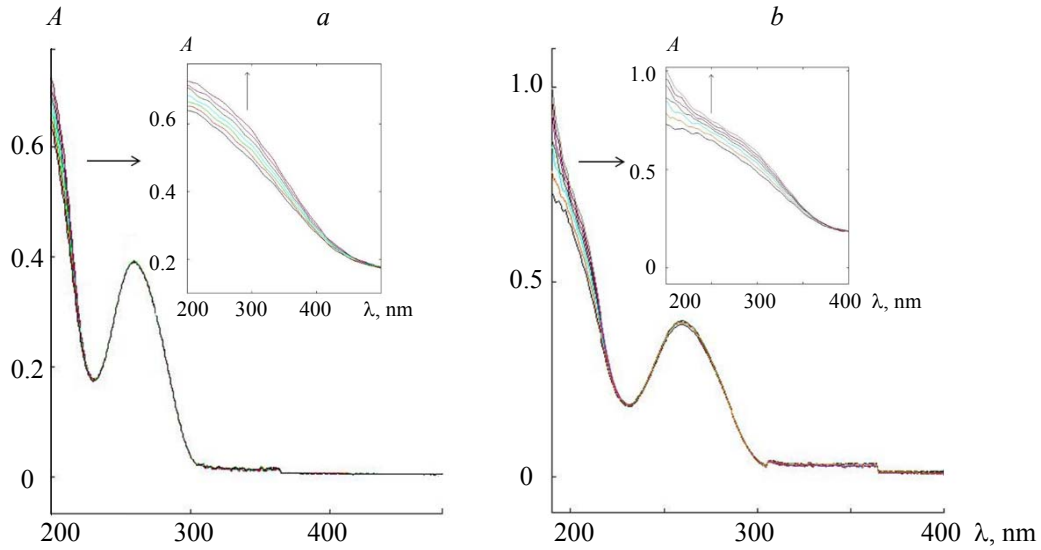

Fig. 7. Change in UV spectra of DNA solution after adding emodin (a) or frangulin-A (b).

Conclusion. In this paper, emodin and frangulin-A were isolated and purified from *Ventilago leiocarpa* Benth. Frangulin-A is a derivative of emodin. Fluorescence spectra and molecular modeling techniques were used. The results showed that emodin and frangulin-A had a strong quenching effect on the BSA endogenous fluorescence. The static quenching and the K_q value of emodin were significantly greater than for frangulin-A. The synchronous spectroscopy of emodin–BSA and frangulin-A–BSA revealed that the BSA conformation had changed. The simulation of molecular docking indicated that emodin and frangulin-A could stably bind with BSA. It forms hydrogen bonds with amino acids, and the amino acids in BSA are involved in the hydrophobic action. According to the UV spectrum, emodin and frangulin-A interact with ct-DNA via electrostatic interaction. The maximum absorption wavelength is redshifted when the concentration increases.

Acknowledgment. This work was financially supported by the Natural Science Foundation of Guangxi Province (2016GXNSFAA380092, 2017GXNSFBA198214), Guangxi Key Laboratory of traditional Chinese Medicine Quality Standards (201506, 201601), and Guangxi Science and Technology Project (AD18216002).

REFERENCES

1. X. F. Wang, W. J. Lu, J. Y. Chen, R. F. Wei, J. Lu, Z. Y. Tian, Q. T. Zheng, *Acta Pharmacol. Sin.*, **2**, 28 (1993).
2. Y. X. Wang, H. Yu, J. Zhang, X. Ge, J. Gao, Y. Y. Zhang, G. Lou, *Cell Oncol.*, **5**, 38 (2015).

3. R. Saleem, S. Faizi, B. S. Siddiqui, M. Ahmed, S. A. Hussain, A. Qazi, A. Dar, S. I. Ahmad, M. H. Qazi, S. Akhtar, S. N. Hasnain, *Planta Med*., **6**, 67 (2001).
4. J. W. Han. *Int. J. Mol. Sci*., **4**, 16 (2015).
5. C. W. Francis, O. Holt, D. W. Aksnes, *Magn. Reson. Chem*., **10**, 36 (1998).
6. S. P. D. Dwivedi, V. B. Pandey, A. H. Shah, Y. B. Rao, *Phytother. Res*., **1**, 2 (2010).
7. I. Rosenthal, E. Wolfram, S. K. Peter, B. Meier, *J. Nat. Prod.*, **3**, 77 (2014).
8. V. A. Kurkin, A. A. Shmygareva, T. K. Ryazanova, A. N. Sankov, *Pharm. Chem. J.*, **7**, 48 (2014).
9. B. L. Wei, C. M. Lu, L. T. Tsao, J. P. Wang, C. N. Lin, *Planta Med*., **8**, 67 (2001).
10. J. Sochacka, A. Sulkowska, A. Kowalska, *Acta Pol. Pharm*., **1**, 65 (2008).
11. S. L. Deng, D. L. Zeng, Y. Luo, J. F. Zhao, X. L. Li, Z. N. Zhao, T. F. Chen, *RSC Adv*., **7**, 27 (2017).
12. D. S. Greene, R. Quintiliani, C. H. Nightingale, *J. Pharm. Sci.*, **11**, 66 (2010).
13. M. R. Eftink, C. A. Ghiron, *Anal. Biochem*., **114**, 199 (1981).
14. M. Zhang, Y. Q. Dang, T. Y. Liu, H. W. Li, Y. Q. Wu, Q. Li, K. Wang, B. Zou, *J. Phys. Chem. C*, **1**, 117 (2013).
15. X. L. Wei, J. B. Xiao, Y. Wang, Y. Bai, *Spectrochim. Acta A*, **1**, 75 (2010).
16. I. Christiaans, T. M. Kok, I. M. V. Langen, E. Birnie, G. J. Bonsel, A. A. M. Wilde, E. M. A. Smets, *Eur. J. Hum. Genet*., **2**, 18 (2010).
17. H. Kai, *Jpn. J. Pharmacol*, **4**, 88 (2002).
18. J. M. Luan, X. D. Zhang, *Phys. Test. Chem. Anal.*, **11**, 42 (2006).
19. C. W. Francis, O. Holt, D. W. Aksnes, *Magn. Reson. Chem*., **10**, 36 (1998).
20. J. Toneatto, G. A. Arguello, *J. Inorg. Biochem*., **5**, 105 (2011).
21. L. Z. Li, Q. Guo, J. F. Dong, T. Xu, J. H. Li, *J. Photoch. Photobiol. B*, **4**, 125 (2013).
22. K. Karami, F. Parsianrad, M. Alinaghi, Z. Amirghofran, *Inorg. Chim. Acta*, **1**, 467 (2017).
23. C. Q. Jiang, M. X. Gao, J. X. He, *Anal. Chim. Acta*, **2**, 452 (2002).
24. Y. Y. Lou, K. L. Zhou, D. Q. Pan, J. L. Shen, J. H. Shi, *J. Photochem. Photobiol. B Biol*., **167** (2017).
25. B. L. Zhang, W. Q. Wang, R. Y. Yao, *Acta Chim. Sin.*, **12**, 52 (1994).
26. L. L. Yu, *Chin. J. Spectrosc. Lab*., **6**, 28 (2011).